DOI 10.1002/mnfr.200700434 Mol. Nutr. Food Res. 2008, *52*, 692 – 700

Research Article

The diet-derived sulforaphane inhibits matrix metalloproteinase-9-activated human brain microvascular endothelial cell migration and tubulogenesis

Borhane Annabi[1]*, Shanti Rojas-Sutterlin[2]*, Mathieu Laroche[2, 3], Marie-Paule Lachambre[2], Robert Moumdjian[3] and Richard Béliveau[2]

[1] Laboratoire d'Oncologie Moléculaire, Département de Chimie, Centre BIOMED, Université du Québec à Montréal, Quebec, Canada
[2] Centre de Cancérologie Charles-Bruneau, Hôpital Sainte-Justine-UQAM, Quebec, Canada
[3] Surgery Department, Neurosurgery Service, Centre Hospitalier de l'Université de Montréal, Quebec, Canada

Human brain microvascular endothelial cells (HBMECs) play an essential role as structural and functional components of the blood–brain barrier (BBB). While disruption of the BBB by the brain tumor-secreted matrix metalloproteinase-9 (MMP-9) favors tumor invasion, the role and regulation of MMP-9 secretion by HBMEC themselves in response to carcinogens or brain tumor-derived growth factors has received little attention. Our study delineates a unique brain endothelial phenotype in that MMP-9 secretion is increased upon phorbol 12-myristate 13-acetate (PMA) treatment of HBMEC. Sulforaphane (SFN), an isothiocyanate present in broccoli which exhibits chemopreventive properties, selectively inhibited the secretion of MMP-9 but not that of MMP-2. The decrease in MMP-9 gene expression correlated with a decrease in the expression of the mRNA stabilizing factor HuR protein triggered by SFN. PMA-induced HBMEC migration was also antagonized by SFN. Silencing of the MMP-9 gene inhibited PMA-induced MMP-9 secretion, cell migration, and *in vitro* tubulogenesis on Matrigel. While SFN inhibited the chemoattractive abilities of brain tumor-derived growth factors, it failed to inhibit PMA-induced tubulogenesis. Our data are indicative of a selective role for SFN to inhibit MMP-9-activated, but not basal, HBMEC migration, and tubulogenesis whose actions could add to SFN's antitumor properties.

Keywords: Brain endothelial cells / Cooption / MMP-9 / Sulforaphane

Received: October 19, 2007; accepted: November 20, 2007

1 Introduction

Tumor angiogenesis was considered, for many years, a vascularization process solely explained by the ingrowth of new vessels into a tumor from pre-existing vessels. With time, tumor angiogenesis became a fast growing subdomain in tumor biology research as basic mechanisms were unraveled and many key players identified [1]. In recent years additional mechanisms, including angioblast recruitment, cooption, vasculogenic mimicry, and mosaic vessels, have been recognized as contributing to tumor vascularization. These different mechanisms may exist concomitantly in the same tumor or may be selectively involved in a specific tumor type or host environment [2]. More recently it has also become clear that tumors may use alternative means of obtaining a blood supply. Vessel cooption, the use of pre-existing vessels, was described first in the brain, one of the most densely vascularized organs in the body. Thus, brain tumors may develop without the need of an angiogenic

Correspondence: Dr. Richard Béliveau, Laboratoire de Médecine Moléculaire, Université du Québec à Montréal, C. P. 8888, Succ. Centre-ville, Montréal, Québec, Canada, H3C 3P8
E-mail: oncomol@nobel.si.uqam.ca
Fax: +1-514-987-0246

Abbreviations: EC, endothelial cell; **EGCg,** epigallocatechin-3-gallate; **HBMEC,** human brain microvascular EC; **IR,** ionizing radiation; **MMP,** matrix metalloproteinase; **PMA,** phorbol 12-myristate 13-acetate; **SFN,** sulforaphane; **TBST,** Tris-buffered saline containing 0.3% Tween-20; **TNF,** tumor necrosis factor

* These authors contributed equally to this work.

switch to occur. Obviously, this means of augmenting blood supply will not be affected by angiogenesis inhibition [3]. Glioblastoma multiforme is, for instance, characterized by exuberant angiogenesis, but the pathologic mechanisms driving the biological behavior of gliomas also involves cooption of native blood vessels [4]. The cerebral endothelium may thus dictate the nature of the brain tumor vascularizing processes and provide a specific environment for therapeutic targeting.

Although the inhibition of tumor angiogenesis is thought to be an efficient therapeutic strategy for the treatment of malignant gliomas [5], the fact that glioma cells can invade the brain diffusely over long distances without necessarily requiring angiogenesis indicates the need for alternative/complementary therapeutic approaches. Furthermore, because systemic antiangiogenic therapy can also apparently increase the invasiveness of gliomas in the orthotopic model, it was concluded that tumor cell invasion is tightly associated with pre-existing blood vessels, confirming that increased cooption of the host vasculature could, in fact, represent a compensatory mechanism that is selected for by inhibiting adequate tumor vascularization [6]. These observations were further strengthened by histologic studies of growth suggesting that these tumors adapt to inhibition of angiogenesis by increased infiltration and cooption of the host vasculature [7]. Targeting tumor-associated endothelial cells (EC) as part of cancer treatments thus becomes an appealing prospect. The expression of matrix metalloproteinases (MMP), particularly MMP-9, is significantly increased during tumor progression and is associated with the opening of the blood–brain barrier (BBB) [8]. Adenoviral-mediated MMP-9 downregulation inhibited human dermal microvascular EC migration in cell wounding and spheroid migration assays, and reduced capillary-like tube formation, demonstrating the key role of MMP-9 in EC network organization [9]. Furthermore, among all MMP, MMP-9 secreted from brain EC has never been investigated and may likely be of importance in brain tumor-associated angiogenesis and become a therapeutic target. A role for MMP-9 in cooption mechanisms remains to be investigated.

Recent reports have proposed that some naturally occurring phytochemicals can function as sensitizers which could, for instance, augment the effectiveness of conventional radiotherapy [10, 11]. Of these phytochemicals, isothiocyanates present in cruciferous vegetables, and particularly sulforaphane (SFN) present in broccoli, are by far the most extensively studied in order to uncover the mechanisms behind its chemopreventive properties [12]. Evidence that SFN acts to inhibit angiogenesis *via* suppression of bovine aortic EC proliferation was recently provided [13, 14]. However, no data are available in the specific targeting of brain tumor-associated EC functions by SFN. Because the human brain microvascular EC (HBMEC) model used in this study, is to our knowledge, the closest *in vitro* surrogate model available that can approximate brain tumor-derived EC phenotype and functions, the goal of our study was to characterize the impact of SFN on the basal and MMP-9-activated phenotype of HBMEC migration and tubulogenesis, with an emphasis on the anti-MMP-9 secretion properties that are attributed to SFN.

2 Materials and methods

2.1 Materials

SDS and BSA were purchased from Sigma (Oakville, ON). Electrophoresis reagents were purchased from BioRad (Mississauga, ON). The enhanced chemiluminescence (ECL) reagents were from Amersham Pharmacia Biotech (Baie d'Urfé, QC). Microbicinchoninic acid protein assay reagents were from Pierce (Rockford, IL). All other reagents were from Sigma–Aldrich (Canada).

2.2 Cell culture

HBMEC were characterized and generously provided by Dr. Kwang Sik Kim from the John Hopkins University School of Medicine (Baltimore, MD). These cells were positive for factor VIII-Rag, carbonic anhydrase IV, and Ulex Europeus Agglutinin I, they took up fluorescently labeled, acetylated low-density lipoprotein and expressed gamma glutamyl transpeptidase, demonstrating their brain EC-specific phenotype [15]. HBMEC were immortalized by transfection with simian virus 40 large T antigen and maintained their morphologic and functional characteristics for at least 30 passages [16]. HBMEC were maintained in RPMI 1640 (Gibco, Burlington, ON) supplemented with 10% v/v inactive fetal bovine serum (iFBS) (HyClone Laboratories, Logan, UT), 10% v/v NuSerum (BD Bioscience, Mountain View, CA), modified Eagle's medium nonessential amino acids (1%) and vitamins (1%) (Gibco), sodium pyruvate (1 mM), and EC growth supplement (30 μg/mL). Culture flasks were coated with 0.2% type-I collagen to support the growth of HBMEC monolayers. Cells were cultured at 37°C under a humidified atmosphere containing 5% CO_2. All experiments were performed using passages 3–28. The HT-1080 cell line was purchased from American Type Culture Collection (Manassas, VI), maintained in Eagle's minimum essential medium (MEM) containing 10% v/v calf serum (HyClone Laboratories), 2 mM glutamine, 100 U/mL penicillin, and 100 mg/mL streptomycin, and cultured at 37°C under a humidified atmosphere containing 5% CO_2.

2.3 RNA interference

RNA interference experiments were performed using Lipofectamine 2000 according to the manufacturer's instructions. A small interfering RNA against human MMP-9 (siMMP-9, GenBank™ accession number NM-004994)

and mismatch siRNA with no known homology to mammalian genes were synthesized (Qiagen, Valencia, CA) against the following published target sequences for MMP-9: 5′-AACATCACCTATTGGATCCAAACTAC-3′, nucleotides 377 – 403 [17], and respectively annealed to form duplexes. The sequence of the siMMP-9 used in this study is as follows: sense siRNA sequence was 5′-CAUCACCUAUUGGAUCCAAdTdT-3′. Antisense siRNA was 5′-UUGGAUCCAAUAGGUGAUGdTdT-3′. Knockdown of MMP-9 expression, as assessed by RT-PCR, ranged routinely from 75 to 90% efficiency.

2.4 cDNA synthesis and real-time quantitative RT-PCR

Total RNA was extracted from cultured HBMEC using the TRIzol reagent (Invitrogen, Burlington, ON). For cDNA synthesis, ~1 μg total RNA was reverse-transcribed into cDNA using Oligo dT primer and iScript cDNA synthesis kit reverse transcriptase. cDNA was stored at −20°C for PCR. MMP-9 gene expression was quantified by real-time quantitative RT-PCR using QuantiTect SYRB Green dye (Qiagen, CA). DNA amplification was carried out using Icycler (Bio-Rad, Hercules, CA), and the detection was performed by measuring the binding of the fluorescence dye SYBR Green I to dsDNA. Primers for MMP-9 (forward: 5′-AAGATGCTGCTGTTCAGCGGG-3′, reverse: 5′-GTCCTCAGGGCACTGCAGGAT-3′) were derived from human sequences. The relative quantities of target gene mRNA against an internal control, 18S ribosomal RNA, was possible by following a ΔC_T method. An amplification plot that had been the plot of fluorescence signal *versus* cycle number was drawn. The difference (ΔC_T) between the mean values in the duplicated samples of target gene and those of 18S ribosomal RNA were calculated by Microsoft Excel and the relative quantified value (RQV) was expressed as $2^{-\Delta C_T}$.

2.5 Analysis of HBMEC migration

HBMEC migration was assessed using modified Boyden chambers. The lower surfaces of Transwells (8-μm pore size; Costar, Acton, MA) were precoated with 0.2% type-I collagen for 2 h at 37°C. The Transwells were then assembled in a 24-well plate (Fisher Scientific, Nepean, ON). The lower chamber was filled with serum-free HBMEC medium or growth factor-enriched conditioned medium isolated from 48 h serum starved U-87 human glioblastoma cells, which we found to exert a very potent chemoattractant effect upon EC migration [18]. Control HBMEC were collected by trypsinization, washed, and resuspended in serum-free medium at a concentration of 10^6 cells/mL; 10^5 cells were then inoculated onto the upper side of each modified Boyden chamber. The plates were placed at 37°C in 5% CO_2/95% air for 30 min after which various concentrations of SFN were added to the lower chambers of the Transwells. Migration then proceeded for 6 h at 37°C in 5% CO_2/95% air. Cells that had migrated to the lower surfaces of the filters were fixed with 10% formalin phosphate and stained with 0.1% crystal violet – 20% methanol v/v. Images of at least five random fields *per* filter were digitized (100 × magnification). The average number of migrating cells *per* field was quantified using Northern Eclipse software (Empix Imaging, Mississauga, ON). Migration data are expressed as a mean value derived from at least four independent experiments.

2.6 EC morphogenesis assay

Tubulogenesis was assessed using Matrigel aliquots of 50 μL, plated into individual wells of 96-well tissue culture plates (Costar, Amherst, MA) and allowed to polymerize at 37°C for 30 min. After brief trypsination, HBMEC were washed and resuspended at a concentration of 10^6 cells/mL in serum-free medium. Next, 25 μL of cell suspension (25 000 cells/well) and 75 μL of medium with serum were added into each culture well. Cells were allowed to form capillary-like tubes at 37°C in 5% CO_2/95% air for 20 h. The formation of capillary-like structures was examined microscopically and pictures (100 ×) were taken using a Retiga 1300 camera (QImaging) and a Nikon Eclipse TE2000-U microscope. The extent to which capillary-like structures formed in the gel was quantified by the analysis of digitized images to determine the thread length of the capillary-like network, using a commercially available image analysis program (Northern Eclipse) as described and validated previously [18, 19]. For each experiment, four randomly chosen areas were quantified by counting the number of tubes formed. Tubulogenesis data are expressed as a mean value derived from at least three independent experiments.

2.7 Gelatin zymography

Gelatin zymography was used to assess the extent of MMP-2 and MMP-9 activity as previously described and validated [20, 21]. Briefly, an aliquot (20 μL) of the culture medium was subjected to SDS-PAGE in a gel containing 0.1 mg/mL gelatin. The gels were then incubated in 2.5% Triton X-100 and rinsed in nanopure distilled H_2O. Gels were further incubated at 37°C for 20 h in 20 mM NaCl, 5 mM $CaCl_2$, 0.02% Brij-35, 50 mM Tris-HCl buffer, pH 7.6, then stained with 0.1% CBB R-250 and destained in 10% acetic acid, 30% methanol in H_2O. Gelatinolytic activity was detected as unstained bands on a blue background.

2.8 Immunoblotting procedures

Cytosolic proteins from control and treated cells were separated by SDS-PAGE. After electrophoresis, proteins were electrotransferred to polyvinylidene difluoride membranes

which were then blocked for 1 h at room temperature with 5% nonfat dry milk in Tris-buffered saline (150 mM NaCl, 20 mM Tris-HCl, pH 7.5) containing 0.3% Tween-20 (TBST). Membranes were further washed in TBST and incubated with the primary polyclonal anti-HuR antibody (1/1000 dilution, Jackson ImmunoResearch Laboratories, West Grove, PA) in TBST containing 3% BSA, followed by a 1 h incubation with horseradish peroxidase-conjugated antirabbit IgG (1/2500 dilution) in TBST containing 5% nonfat dry milk. Immunoreactive material was visualized by enhanced ECL (Amersham Biosciences).

2.9 Fluorimetric caspase-3 activity assay

HBMEC were grown to 60% confluence and treated with increasing concentrations of SFN. Cells were collected and washed in ice-cold PBS pH 7.0. Cells were subsequently lysed in Apo-Alert lysis buffer (Clontech, Palo Alto, CA) for 1 h at 4°C and the lysates were clarified by centrifugation at 16 000 × *g* for 20 min. Caspase-3 activity was determined by incubation with 50 μM of the caspase-3-specific fluorogenic peptide substrate acetyl-Asp-Glu-Val-Asp-7-amino-4-trifluoromethylcoumarin (Ac-DEVD-AFC) in assay buffer (50 mM Hepes–NaOH (pH 7.4), 100 mM NaCl, 10% sucrose, 0.1% 3-[(3-cholamidopropyl)dimethylammonio]-1-propanesulfonate, 5 mM DTT and 1 mM EDTA) in 96-well plates [22]. The release of AFC was monitored for at least 30 min at 37°C on a fluorescence plate reader (Molecular Dynamics) (λ_{ex} = 400 nm, λ_{em} = 505 nm).

2.10 Statistical data analysis

Data are representative of three or more independent experiments. Statistical significance was assessed using Student's unpaired *t*-test and probability values of less than 0.05 were considered significant; an asterisk (*) identifies such significance in each figure.

3 Results

3.1 MMP-9 secretion is selectively induced by phorbol 12-myristate 13-acetate (PMA) and inhibited by SFN

We first assessed HBMECs' response to the inflammatory mediator tumor necrosis factor (TNF)-α and to the carcinogen PMA, two well established MMP-9 secretion inducers [23]. Cells were serum-starved, treated for 18 h and conditioned media was harvested to measure MMP levels by gelatin zymography. While MMP-2 extracellular levels remained unaffected, those of MMP-9 were increased in PMA-treated cells but not upon TNF treatment (Fig. 1A). In contrast, both PMA and TNF-induced MMP-9 secretion in HT-1080 fibrosarcoma cells. When HBMEC were

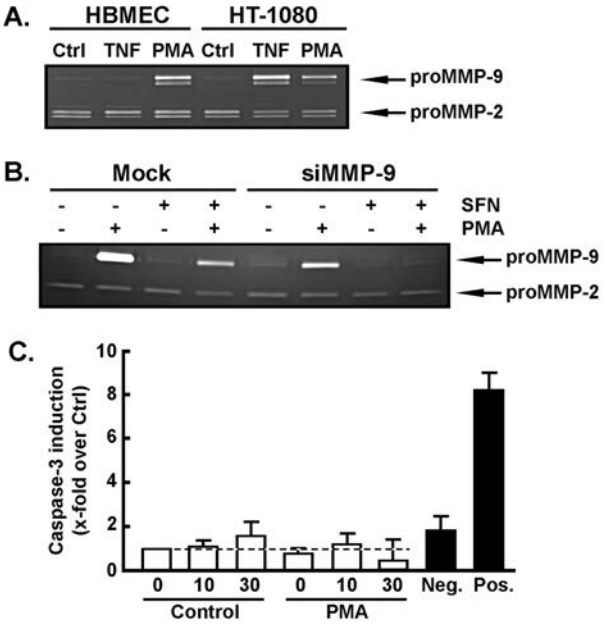

Figure 1. MMP-9 secretion is selectively induced by PMA and inhibited by SFN. HBMEC and HT-1080 fibrosarcoma cell lines were cultured as described in Section 2. (A) Cells were then serum-starved in the presence or absence of 1 ng/mL TNF or 1 μM PMA for 18 h. Conditioned media was then harvested and gelatin zymography performed in order to detect proMMP-9 and proMMP-2 hydrolytic activity. (B) In order to downregulate MMP-9 gene expression, control HBMEC (Mock) or HBMEC were transfected with either a mismatched or a specific siRNA (siMMP-9) as described in Section 2. Cells were then serum-starved in the presence of 1 μM PMA, 10 μM SFN, or a combination of both for 18 h. Conditioned media was harvested and gelatin zymography performed in order to detect proMMP-9 and proMMP-2 hydrolytic activity. (C) Caspase-3 activity was measured as described in Section 2 in order to evaluate the potential cytotoxic effects of SFN. Caspase-3 activity upon treatment with 10 and 30 μM SFN is shown for control and PMA-treated cells. A negative (Neg.) and a positive (Pos.) internal control for the assay were provided and consisted of marrow stromal cell lysates treated or not with the proapoptotic cytoskeleton disrupting agent Concanavalin-A [43].

treated with combined PMA and SFN, MMP-9 was found to be significantly inhibited (Fig. 1B). When MMP-9 gene expression was silenced using siRNA strategies, PMA induction of MMP-9 was significantly reduced and SFN completely inhibited PMA-induced MMP-9 secretion (Fig. 1B), indicating a role of SFN in the inhibition of MMP-9 gene expression upon PMA signaling. Moreover, we assessed cell viability through caspase-3 activity in cells treated with up to 30 μM SFN and found no deleterious effect on HBMEC viability (Fig. 1C). Collectively, these results suggest that selective MMP-9 gene expression affects extracellular MMP-9 levels in response to tumor promoting conditions rather than to inflammatory mediators in HBMEC.

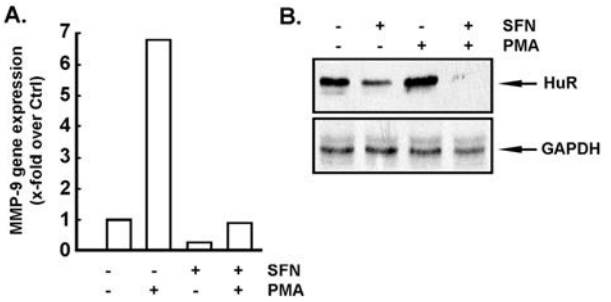

Figure 2. Reduction of MMP-9 transcripts by SFN correlates with an effect on HuR protein expression. (A) In order to confirm the zymography data obtained in Fig. 1 for the MMP-9 gelatinolytic activity, HBMEC were cultured in the presence of 10 μM SFN, 1 μM PMA, or a combination of both, total RNA isolated and MMP-9 gene expression assessed by qRT-PCR as described in Section 2. (B) In parallel experiments, the cytosolic fraction of these same cells were isolated as described in ref. [44], and HuR protein expression assessed by Western blotting. GAPDH expression was used as an internal house keeping gene control.

3.2 SFN inhibits PMA-induced HuR protein and MMP-9 gene expression in HBMEC

Although most published studies have focused on the transcriptional control of MMP-9 expression, there is increasing evidence that its expression can also be regulated at the levels of mRNA stability, translation, and protein secretion. Among the factors shown to stabilize MMP-9 mRNA and augment its expression [24], HuR has been ascribed a pivotal role in the development of tumors [25] and been found to be a key mediator during macrophage activation in PMA-differentiated HL-60 cells [20]. We next tested whether SFN affected MMP-9 transcripts levels and whether any MMP-9 modulation could be correlated to that of cytosolic HuR protein expression. Total RNA was isolated from treated HBMEC, and MMP-9 gene expression assessed by quantitative RT-PCR. PMA was found to increase MMP-9 gene expression, while SFN was able to antagonize that increase as well as in untreated cells (Fig. 2A). The protein expression of HuR was also assessed in those same conditions and found to be decreased by SFN in the cytosolic fraction where it is reported to exert MMP-9 mRNA stabilization, while that of GAPDH remained unaffected (Fig. 2B). Collectively, insight into the anti-MMP-9 effect of SFN may involve downregulation of HuR which may ultimately decrease MMP-9 mRNA stability.

3.3 SFN antagonizes PMA-induced MMP-9 secretion and MMP-9-dependent cell migration in HBMEC

The effects of SFN on MMP-9 secretion and on cell migration were further investigated. We found a dose-dependent inhibition of MMP-9 secretion in PMA-treated HBMEC,

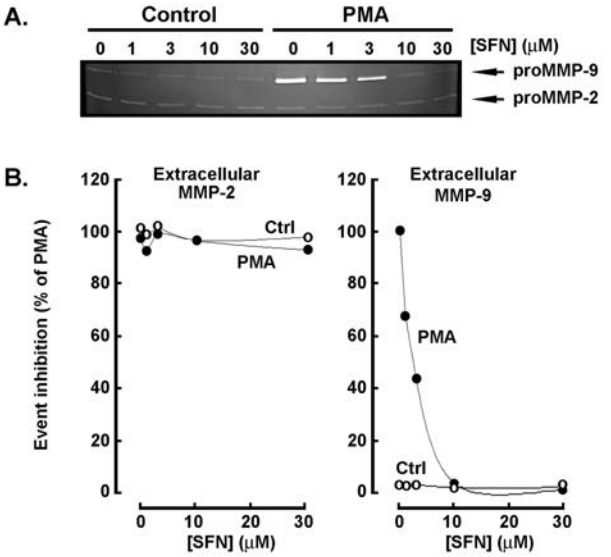

Figure 3. SFN specifically antagonizes PMA-induced proMMP-9 secretion in HBMEC. HBMEC were serum-starved in the presence of increasing concentrations of SFN in combination with (or lacking) 1 μM PMA for 18 h. (A) Conditioned media was then harvested and gelatin zymography performed in order to detect proMMP-9 and proMMP-2 hydrolytic activity as described in Section 2. (B) Scanning densitometry was used to quantify the extent of either proMMP-2 gelatin hydrolysis (left panel), or proMMP-9 gelatin hydrolysis (right panel). Data shown are representative from three independent experiments.

while MMP-2 extracellular levels remained unaffected (Fig. 3A). SFN almost completely inhibited PMA-induced MMP-9 secretion at 10 μM, with a calculated IC_{50} of 1 – 3 μM (Fig. 3B, right panel). MMP-2 secretion remained unaffected in all conditions (Fig. 3B, left panel), demonstrating SFN's specificity of action. Cell migration was also induced by PMA in HBMEC while SFN dose-dependently inhibited such migration with an IC_{50} ranging from 0.3 to 1 μM (Fig. 4A). Interestingly, SFN specifically targeted the migration of PMA-treated HBMEC but not that of untreated cells (Fig. 4A). Gene silencing of MMP-9 combined with SFN treatment of HBMEC further highlighted the importance of MMP-9 in HBMEC migration, since PMA was unable to efficiently trigger cell migration in cells where MMP-9 levels were reduced by silencing (Fig. 4B). The effects of SFN on PMA-induced cell migration and MMP-9 secretion were further plotted and showed a very nice correlation ($r^2 = 0.985$, Fig. 4C) demonstrating that the more PMA-induced MMP-9 secretion is inhibited, the more PMA-induced cell migration is as well.

3.4 SFN inhibits HBMEC migration in response to brain tumor-derived growth factors

In addition to its inhibitory effect against carcinogen-induced HBMEC migration, we assessed SFN's capacity to

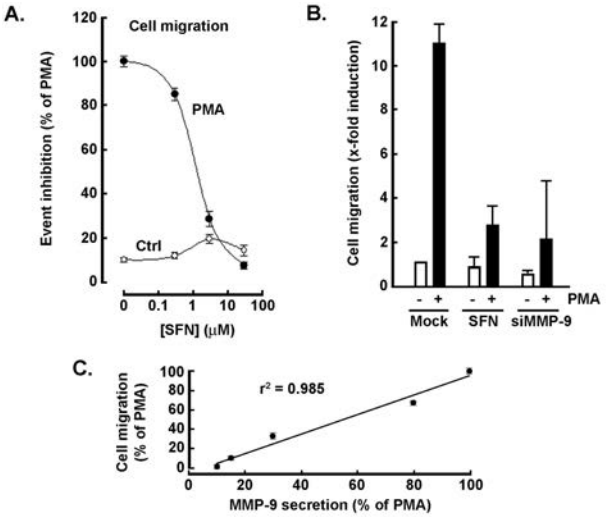

Figure 4. SFN specifically antagonizes PMA-induced HBMEC migration. (A) HBMEC migration was assessed in modified Boyden chambers using control (open circles) and PMA-treated cells (closed circles). Both were concomitantly treated with various SFN concentrations. At the end of the treatment, cells were harvested and 10^6 cells seeded on top of gelatin-coated filters. Migration proceeded for 6 h. (B) Untransfected (Mock) cells were treated with or without 10 μM SFN, 1 μM PMA, or a combination of both for 16 h. HBMEC migration was then compared to that of cells transfected with a specific MMP-9 siRNA. (C) The effects of different concentrations of SFN upon PMA-induced cell migration and PMA-induced MMP-9 secretion were plotted and linear regression curve calculated.

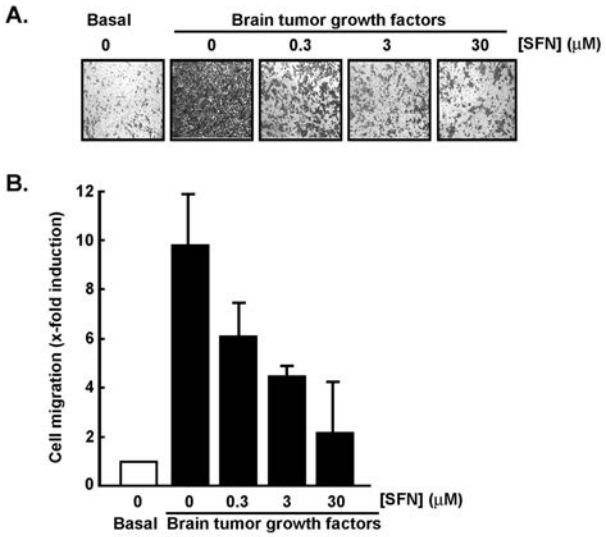

Figure 5. SFN inhibits HBMEC migration in response to brain tumor-derived growth factors. (A) HBMEC migration was assessed in response to brain tumor-derived growth factors conditioned media, isolated from serum-starved U-87 glioma cells, and that served as chemoattractant. In addition, various concentrations of SFN were added to the chemoattractant; cell migration was proceeded for 6 h and (B) was quantified.

affect HBMEC migration in response to conditioned media generated from serum-starved subconfluent U87 glioblastoma cell cultures [18] and that is enriched in brain tumor-derived growth factors. HBMEC migration was efficiently induced up to ten-fold by tumor-derived growth factors chemoattraction (Fig. 5A). This chemoattracting effect was dose-dependently decreased when SFN was added to the lower chamber of migration (Fig. 5B). This suggests that SFN potentially inhibits some intracellular signaling pathways triggered in response to tumor growth factors.

3.5 MMP-9 is involved in 3-D capillary-like structure formation by HBMEC

The importance of MMP-9 in HBMEC tubulogenesis was assessed in mock-transfected and siMMP-9-transfected cells. We observed that, as expected for differentiated ECs, HBMEC formed well-defined, capillary-like structures on Matrigel (Fig. 6A). While PMA treatment induced *in vitro* tubulogenesis, transient gene silencing of MMP-9 decreased basal HBMEC tube formation suggesting that MMP-9-mediated events were crucial for tubulogenesis, while PMA was found unable to trigger HBMEC tube formation in siMMP-9 cells in comparison to Mock cells (Fig. 6B). This suggests that MMP-9, most probably both the soluble fraction and the fraction bound to the cell surface of HBMEC, is actively involved in tubulogenesis.

3.6 SFN selectively inhibits *in vitro* capillary-like structure formation in MMP-9-activated HBMEC

Because SFN selectively inhibited PMA-induced MMP-9 secretion and PMA-induced HBMEC migration, we also evaluated whether it might inhibit HBMEC tubulogenesis. Cells were seeded on top of Matrigel and left to adhere as described in Section 2. SFN or the green tea-derived catechin epigallocatechin-3-gallate (EGCg), an antiangiogenic molecule that we have shown to inhibit MMP-9 secretion [20], and to sensitize HBMEC to ionizing radiation (IR) [22], were then added to the wells and the extent of tubulogenesis assessed (Fig. 7A). We found that 10 μM SFN was unable to inhibit basal (white bars) capillary-like structure formation, while it reduced by ~45% PMA-induced (black bars) *in vitro* tubulogenesis (Fig. 7B). In contrast, EGCg efficiently inhibited both basal and PMA-induced tubulogenesis. This observation suggests that, in addition to its activity against cell migration and ECM degradation, SFN specifically targets the MMP-9-dependent tubulogenesis of HBMEC.

4 Discussion

The transformation of the regular vasculature in normal tissue into a highly heterogeneous tumor capillary network is

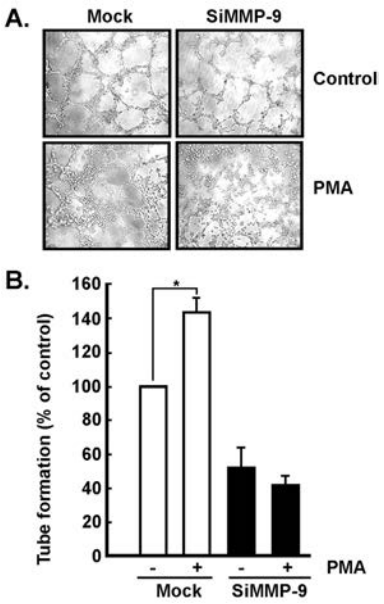

Figure 6. MMP-9 is involved in three-dimensional capillary-like structure formation by HBMEC. (A) In order to assess *in vitro* tubulogenesis, untransfected (Mock), or siMMP-9-transfected (siMMP-9) HBMEC were treated with or without 1 μM PMA and seeded on top of Matrigel for 16 h. (B) The extent of 3-D capillary-like structure formation was assessed as described in Section 2 for Mock (white bars) and siMMP-9-transfected (black bars) HBMEC. (*) depicts statistical significance ($p < 0.05$).

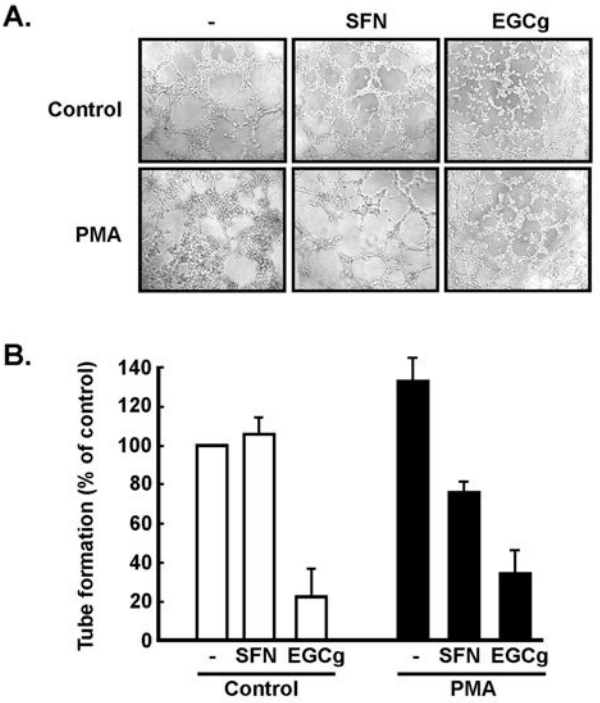

Figure 7. SFN preferentially inhibits *in vitro* capillary-like structure formation in MMP-9 activated HBMEC. (A) The extent of capillary-like structure formation was assessed as described in Section 2 for control and PMA-treated HBMEC, in the presence of 10 μM SFN or 10 μM EGCg. (B) Tube formation was quantified in basal (white bars) and MMP-9-activated (black bars) HBMEC as described in Section 2.

described by models incorporating tumor growth, vessel cooption, neovascularization, vessel collapse, and cell death [26]. Although different mechanisms of tumor vascularization have been characterized, much is unknown about their interaction with diet-derived molecules. The combined tumor vascularizing processes in tumor development, in fact, render difficult their specific targeting in antitumor therapy. Brain tumors are highly vascularized and, at early stages of development, tumor-associated vessels possess a phenotype similar to that in their normal brain environment. This phenotype can, in fact, explain why it is difficult to detect gliomas at early stages by MRI analysis [3]. While brain tumors can use angiogenesis to develop in a highly vascularized tissue such as brain, they can also use alternate vascularization mechanisms such as cooption [27]. In the present study, the specific targeting of the molecular players involved in brain EC cooption increases our comprehension of the chemopreventive properties of SFN. Collectively, we provide evidence that the almost complete (>90%) inhibition of MMP-9-activated, but not basal, HBMEC migration in comparison to the less potent inhibition (~45%) of tubulogenesis may highlight a potential role of SFN against cooption mechanisms.

Recently it was shown that EC, isolated from tumors, grew independent of the presence of endothelial growth factors, suggesting that tumor EC acquire some characteristics that make them less sensitive to antiangiogenic therapy [28]. This finding prompted the search for alternate antitumor molecules that can target cooption mechanisms, such as the SFN differential targeting of HBMEC migration that we report here. Because cooption also depends on the site of tumor development, the specific host–tumor interaction in brain can therefore be considered to dictate the vascular endothelium behavior and could explain why SFN possesses antiangiogenic activity in umbilical- or dermal-derived EC but not in cerebral EC. Antiangiogenic agents have thus far been used with some success [29, 30], but mostly in combination with IR to increase their therapeutic efficacy [31, 32]. Only recently have the brain EC been considered not only as the target of antiangiogenic agents but also of IR, therefore representing a powerful new potential treatment target in highly vascularized tumors such as glioblastoma [18, 33]. In line with this, EGCg, a green tea-derived molecule, has been recognized as having many antitumor biochemical functions including inhibition of tumor cell growth and of angiogenesis [34]. Furthermore, we have recently shown that EGCg suppressed MMP-9 secretion [20] and vascular endothelial growth factor receptor function in EC [19], and that EGCg efficiently targeted those human EC that escaped IR-induced damage [18, 22]. Given

that HuR levels are elevated in cancer [35], and have a pivotal role in promoting angiogenesis [36, 37], we also found, in line with the anti-MMP-9 gene expression effect of SFN, that inhibition of HuR expression by EGCg efficiently suppressed PMA-induced MMP-9 secretion in promyelocytic leukemia cells [20]. It is thus tempting to suggest that inhibition of HuR-regulated expression of markers, such as MMP-9 by EGCg or SFN, could be potential targets of anticancer nutraceutical molecules.

In order to further document the chemopreventive properties of SFN, we show in our study that SFN may represent such a class of molecules that could effectively target MMP-9-mediated brain EC migration properties independent of EC angiogenesis. This finding complements the major mechanism by which SFN acts and that includes suppression of cytochrome P450 enzymes, induction of apoptotic pathways, suppression of cell cycle progression, and anti-inflammatory activity [12]. SFN has been shown to act as a histone deacetylase inhibitor preventing NFkB activation [38]. Given that PMA triggers NFkB activation which, in turn, induces MMP-9 transcription [39], one can hypothesize that inhibition of histone deacetylase by SFN in HBMEC may also play a role in MMP-9 inhibition. The specific phenotype of differentiated HBMEC dictates its specific response to SFN. As such, SFN was shown to suppress 12-*O*-tetradecanoylphorbol-13-acetate (TPA)-induced cancer cell invasion and MMP-9 activity in human MDA-MB-231 breast cancer cells [40], while others have shown that SFN did not affect MMP production in human umbilical vein ECs (HUVECs) as a model of angiogenesis but still inhibited tube formation on Matrigel [41]. SFN also potently decreased newly formed microcapillaries in a human *in vitro* antiangiogenesis model with an IC_{50} of 0.08 μM [13], a value that is very close to the IC_{50} for MMP-9 secretion inhibition that we observed in this study. Furthermore, daily administration of SFN (100 nmol/day, intravenously for 7 day) to female Balb/c mice bearing VEGF-impregnated Matrigel plugs strongly and significantly suppressed angiogenesis progression [14]. These findings, combined with ours, suggest that the EC population is a target of SFN action both *in vitro* and *in vivo*. SFN may thus interfere with all essential steps of neovascularization targeting angiogenesis as well as with cooption mechanisms within specific tissues where EC proliferation, migration, and tube formation occur.

In conclusion, angiogenic inhibitors are increasingly used in combination with chemotherapy in experimental mouse models and in medical therapy [42]. One explanation for the benefits of this combination is that antiangiogenic therapy normalizes the tumor vasculature by shutting-down nonfunctional blood vessels, but still permits alternate vascularization processes to take place. Our study provides molecular evidence for diet-derived molecules such as SFN to further target those brain EC involved in cooption mechanisms and highlights a potential role for SFN to inhibit MMP-9-mediated functions in HBMEC.

B. A. holds a Canada Research Chair in Molecular and Metabolic Oncology from the Canadian Institutes of Health Research (CIHR). R. B. holds both an Institutional UQAM Research Chair in Cancer Prevention and Treatment and the Claude Bertrand Chair in Neurosurgery (CHUM).

The authors have declared no conflict of interest.

5 References

[1] Harper, J., Moses, M. A., Molecular regulation of tumor angiogenesis: Mechanisms and therapeutic implications. *EXS* 2006, *96*, 223 – 268.

[2] Auguste, P., Lemiere, S., Larrieu-Lahargue, F., Bikfalvi, A., Molecular mechanisms of tumor vascularization. *Crit. Rev. Oncol. Hematol.* 2005, *54*, 53 – 61.

[3] Leenders, W. P., Kusters, B., de Waal, R. M., Vessel co-option: How tumors obtain blood supply in the absence of sprouting angiogenesis. *Endothelium* 2002, *9*, 83 – 87.

[4] Fischer, I., Gagner, J. P., Law, M., Newcomb, E. W., Zagzag, D., Angiogenesis in gliomas: Biology and molecular pathophysiology. *Brain Pathol.* 2005, *15*, 297 – 310.

[5] Tuettenberg, J., Friedel, C., Vajkoczy, P., Angiogenesis in malignant glioma – a target for antitumor therapy? *Crit. Rev. Oncol. Hematol.* 2006, *59*, 181 – 193.

[6] Lamszus, K., Kunkel, P., Westphal, M., Invasion as limitation to anti-angiogenic glioma therapy. *Acta Neurochir. Suppl.* 2003, *88*, 169 – 177.

[7] Rubenstein, J. L., Kim, J., Ozawa, T., Zhang, M., *et al*., Anti-VEGF antibody treatment of glioblastoma prolongs survival but results in increased vascular cooption. *Neoplasia* 2000, *2*, 306 – 314.

[8] Shigemori, Y., Katayama, Y., Mori, T., Maeda, T., Kawamata, T., Matrix metalloproteinase-9 is associated with blood-brain barrier opening and brain edema formation after cortical contusion in rats. *Acta Neurochir. Suppl*. 2006, *96*, 130 – 133.

[9] Jadhav, U., Chigurupati, S., Lakka, S. S., Mohanam, S., Inhibition of matrix metalloproteinase-9 reduces *in vitro* invasion and angiogenesis in human microvascular endothelial cells. *Int. J. Oncol.* 2004, *25*, 1407 – 1414.

[10] Chendil, D., Ranga, R. S., Meigooni, D., Sathishkumar, S., Ahmed, M. M., Curcumin confers radiosensitizing effect in prostate cancer cell line PC-3. *Oncogene.* 2004, *23*, 1599 – 1607.

[11] Baatout, S., Derradji, H., Jacquet, P., Mergeay, M., Increased radiation sensitivity of an eosinophilic cell line following treatment with epigallocatechin-gallate, resveratrol and curcuma. *Int. J. Mol. Med.* 2005, *15*, 337 – 352.

[12] Juge, N., Mithen, R. F., Traka, M., Molecular basis for chemoprevention by sulforaphane: A comprehensive review. *Cell. Mol. Life Sci.* 2007, *64*, 1105 – 1127.

[13] Bertl, E., Bartsch, H., Gerhauser, C., Inhibition of angiogenesis and endothelial cell functions are novel sulforaphane-mediated mechanisms in chemoprevention. *Mol. Cancer Ther*. 2006, *5*, 575 – 585.

[14] Jackson, S. J., Singletary, K. W., Venema, R. C., Sulforaphane suppresses angiogenesis and disrupts endothelial mitotic progression and microtubule polymerization. *Vascul. Pharmacol.* 2007, *46*, 77 – 84.

[15] Stins, M. F., Gilles, F., Kim, K. S., Selective expression of adhesion molecules on human brain microvascular endothelial cells. *J. Neuroimmunol*. 1997, *76*, 81 – 90.

[16] Greiffenberg, L., Goebel, W., Kim, K. S., Weiglein, I., *et al*., Interaction of Listeria monocytogenes with human brain microvascular endothelial cells: InlB-dependent invasion, long-term intracellular growth, and spread from macrophages to endothelial cells. *Infect. Immun*. 1998, *66*, 5260 – 5267.

[17] Deryugina, E. I., Zijlstra, A., Partridge, J. J., Kupriyanova, T. A., *et al.*, Unexpected effect of matrix metalloproteinase down-regulation on vascular intravasation and metastasis of human fibrosarcoma cells selected in vivo for high rates of dissemination. *Cancer Res*. 2005, *65*, 10959 – 10969.

[18] McLaughlin, N., Annabi, B., Kim, K. S., Bahary, J. P., *et al.*, The response to brain tumor-derived growth factors is altered in radioresistant human brain endothelial cells. *Cancer Biol. Ther.* 2006, *5*, 1539 – 1545.

[19] Lamy, S., Gingras, D., Beliveau, R., Green tea catechins inhibit vascular endothelial growth factor receptor phosphorylation. *Cancer Res.* 2002, *62*, 381 – 385.

[20] Annabi, B., Currie, J. C., Moghrabi, A., Beliveau, R., Inhibition of HuR and MMP-9 expression in macrophage-differentiated HL-60 myeloid leukemia cells by green tea polyphenol EGCg. *Leuk. Res*. 2007, *31*, 1277 – 1284.

[21] Annabi, B., Lachambre, M. P., Bousquet-Gagnon, N., Page, M., *et al.*, Green tea polyphenol (–)-epigallocatechin 3-gallate inhibits MMP-2 secretion and MT1-MMP-driven migration in glioblastoma cells. *Biochim. Biophys. Acta* 2002, *1542*, 209 – 220.

[22] McLaughlin, N., Annabi, B., Lachambre, M. P., Kim, K. S., *et al.*, Combined low dose ionizing radiation and green tea-derived epigallocatechin-3-gallate treatment induces human brain endothelial cells death. *J. Neurooncol*. 2006, *80*, 111 – 121.

[23] Hetzel, M., Walcher, D., Grub, M., Bach, H., *et al.*, Inhibition of MMP-9 expression by PPARgamma activators in human bronchial epithelial cells. *Thorax* 2003, *58*, 778 – 783.

[24] Akool, el-S., Kleinert, H., Hamada, F. M., Abdelwahab, M. H., *et al.*, Nitric oxide increases the decay of matrix metalloproteinase 9 mRNA by inhibiting the expression of mRNA-stabilizing factor HuR. *Mol. Cell. Biol.* 2003, *23*, 4901 – 4916.

[25] Audic, Y., Hartley, R. S., Post-transcriptional regulation in cancer. *Biol. Cell.* 2004, *96*, 479 – 498.

[26] Bartha, K., Rieger, H., Vascular network remodeling via vessel cooption, regression and growth in tumors. *J. Theor. Biol.* 2006, *241*, 903 – 918.

[27] Holash, J., Maisonpierre, P. C., Compton, D., Boland, P., *et al.*, Vessel cooption, regression, and growth in tumors mediated by angiopoietins and VEGF. *Science* 1999, *284*, 1994 – 1998.

[28] Bussolati, B., Deambrosis, I., Russo, S., Deregibus, M. C., Camussi, G., Altered angiogenesis and survival in human tumor-derived endothelial cells. *FASEB J.* 2003, *17*, 1159 – 1161.

[29] Reardon, D. A., Wen, P. Y., Therapeutic advances in the treatment of glioblastoma: Rationale and potential role of targeted agents. *Oncologist* 2006, *11*, 152 – 164.

[30] Simpson, L., Galanis, E., Recurrent glioblastoma multiforme: Advances in treatment and promising drug candidates. *Expert Rev. Anticancer Ther.* 2006, *6*, 1593 – 1607.

[31] Schuuring, J., Bussink, J., Bernsen, H. J., Peeters, W., van Der Kogel, A. J., Irradiation combined with SU5416: Microvascular changes and growth delay in a human xenograft glioblastoma tumor line. *Int. J. Radiat. Oncol. Biol. Phys.* 2005, *61*, 529 – 534.

[32] Stupp, R., Mason, W. P., van der Bent, M. J., Weller, M., *et al*., European Organisation for Research and Treatment of Cancer Brain Tumor and Radiotherapy Groups; National Cancer Institute of Canada Clinical Trials Group. Radiotherapy plus concomitant and adjuvant temozolomide for glioblastoma. *N. Engl. J. Med.* 2005, *352*, 987 – 996.

[33] Yuan, H., Gaber, M. W., Boyd, K., Wilson, C. M., *et al.*, Effects of fractionated radiation on the brain vasculature in a murine model: Blood-brain barrier permeability, astrocyte proliferation, and ultrastructural changes. *Int. J. Radiat. Oncol. Biol. Phys.* 2006, *66*, 860 – 866.

[34] Demeule, M., Michaud-Levesque, J., Annabi, B., Gingras, D., *et al.*, Green tea catechins as novel antitumor and antiangiogenic compounds. *Curr. Med. Chem. Anticancer Agents* 2002, *2*, 441 – 463.

[35] Lopez de Silanes, I., Fan, J., Galban, C. J., Spencer, R. G., *et al*., Global analysis of HuR-regulated gene expression in colon cancer systems of reducing complexity. *Gene Expr.* 2004, *12*, 49 – 59.

[36] Levy, N. S., Chung, S., Furneaux, H., Levy, A. P., Hypoxic stabilization of vascular endothelial growth factor mRNA by the RNA-binding protein HuR. *J. Biol. Chem.* 1998, *273*, 6417 – 6423.

[37] Sheflin, L. G., Zou, A. P., Spaulding, S. W., Androgens regulate the binding of endogenous HuR to the AU-rich 3'UTRs of HIF-1alpha and EGF mRNA. *Biochem. Biophys. Res. Commun.* 2004, *322*, 644 – 651.

[38] Myzak, M. C., Dashwood, R. H., Histone deacetylases as targets for dietary cancer preventive agents: Lessons learned with butyrate, diallyl disulfide, and sulforaphane. *Curr. Drug Targets* 2006, *7*, 443 – 452.

[39] Shin, Y., Yoon, S. H., Choe, E. Y., Cho, S. H., *et al.*, PMA-induced up-regulation of MMP-9 is regulated by a PKC alpha-NF-kappaB cascade in human lung epithelial cells. *Exp. Mol. Med*. 2007, *39*, 97 – 105.

[40] Rose, P., Huang, Q., Ong, C. N., Whiteman, M., Broccoli and watercress suppress matrix metalloproteinase-9 activity and invasiveness of human MDA-MB-231 breast cancer cells. *Toxicol. Appl. Pharmacol*. 2005, *209*, 105 – 113.

[41] Asakage, M., Tsuno, N. H., Kitayama, J., Tsuchiya, T., *et al.*, Sulforaphane induces inhibition of human umbilical vein endothelial cells proliferation by apoptosis. *Angiogenesis* 2006, *9*, 83 – 91.

[42] Erber, R., Thurnher, A., Katsen, A. D., Groth, G., *et al.*, Combined inhibition of VEGF and PDGF signaling enforces tumor vessel regression by interfering with pericyte-mediated endothelial cell survival mechanisms. *FASEB J.* 2004, *18*, 338 – 340.

[43] Annabi, B., Thibeault, S., Lee, Y. T., Bousquet-Gagnon, N., *et al.*, Matrix metalloproteinase regulation of sphingosine-1-phosphate-induced angiogenic properties of bone marrow stromal cells. *Exp. Hematol.* 2003, *31*, 640 – 649.

[44] Lanthier, J., Desrosiers, R. R., Regulation of protein L-isoaspartyl methyltransferase by cell-matrix interactions: Involvement of integrin alphavbeta3, PI 3-kinase, and the proteasome. *Biochem. Cell. Biol.* 2006, *84*, 684 – 694.

